

Understanding the approach to thermalization in a non-Abelian gauge theory

Sayak Guin^{a,*}, Harshit Pandey^a, Sayantan Sharma^a

^aThe Institute of Mathematical Sciences, a CI of Homi Bhabha National Institute, Chennai, 60113, India

Abstract

We measure the maximal Lyapunov exponent λ_L of physical states in a SU(2) gauge theory both in and out-of-thermal equilibrium conditions using ab-initio lattice techniques. A non-equilibrium state is realized starting from an over-occupied initial condition for low momentum, soft gluons whereas the thermal state comprises of strongly interacting soft gluons at temperatures where these are well separated from the hard momentum modes. A spectra of positive Lyapunov exponents is observed in both these states, similar to a chaotic dynamical system. From the Kolmogorov-Sinai entropy rate measured in terms of this spectrum, we estimate the typical time-scale of $\sim 0.50(3)$ fm/c to achieve thermalization at $T \sim 600$ MeV starting from the non-thermal state. We also measure, for the first time, the λ_L for long wavelength critical modes of SU(2) using the out-of-time-ordered correlation functions of a classical Z_2 scalar field theory, which shares the same universal behavior near the deconfinement phase transition. The λ_L is observed to maximize at the transition temperature.

Keywords: Non-equilibrium quantum field theory, QCD, non-Abelian gauge theory, chaos, out-of-time-ordered correlation

1. Motivation

Understanding the mechanism of thermalization in strongly interacting systems is a challenging research problem in theoretical physics [1, 2] as it would be able to explain physics at different length scales, e.g. in heavy-ion collisions, cold atom traps or in the early universe. Starting from a non-equilibrium state, a necessary condition for eventually reaching a thermal state is a mixing between different regions of the phase space. A mixing in the phase space can occur if there is a mechanical instability in the system [3], which is characterized by at least one positive Lyapunov exponent. Furthermore in the thermal state the entropy or the information content [4] is maximized [5]. Except for a few simple systems [6, 7] it is not very well understood how the entropy evolves as a function of time, starting from a chaotic non-equilibrium state and eventually maximizing itself in a thermal state. One important observable is the rate of change of entropy, known as the Kolmogorov-Sinai (KS) entropy rate [8], which equals the sum of all positive Lyapunov exponent for Hamiltonian systems [9]. This is known to be true for dissipative systems that has an attractor solution. Hence calculating the Lyapunov exponents in chaotic dynamical systems is crucial to understand if, and in what time-scales these would eventually thermalize.

In this Letter, we revisit the question whether non-Abelian gauge theories are chaotic dynamical systems [10, 11, 12], however with a goal to understand the phase space mixing and the process of entropy maximization in an interacting quantum field theory. For this purpose, we measure the maximal Lyapunov exponent of 3 dimensional SU(2) gauge theory using ab-initio lattice techniques in three distinct regimes; for a particular non-thermal classical attractor state [13, 14] and for thermal

states near to the color-deconfinement phase transition and at high temperatures, deep in the deconfined phase. Measuring the KS entropy rate in a typical thermal state at ~ 600 MeV from the Lyapunov exponents, we for the first time provide an estimate of the typical thermalization time $\sim 0.50(3)$ fm/c for the system to relax into it, starting from the classical attractor regime. This estimate is consistent with the recently reported result [15] for the thermalization time measured in terms of the evolution of the scale that characterizes the infrared magnetic modes of QCD starting from the same non-thermal state. Apart from reinforcing the stochastic features of non-Abelian gauge theories [16] already strongly developed in its classical modes, our study has a practical relevance as well. It provides an estimate of how long it takes to achieve local thermal equilibration i.e. to evolve to a quark gluon plasma phase with initial temperatures 300-600 MeV starting from a highly occupied gluon (glasma) phase believed to be formed in the early stages of a typical heavy-ion collision event [17].

2. Theoretical background

We begin with a discussion about how to measure the (maximal) Lyapunov exponent in a non-Abelian SU(2) gauge theory which is a non-linear quantum field theory. We recall that in a classical dynamical system, starting from two closely spaced initial coordinates and performing a Hamiltonian evolution if the separation between the two trajectories increases exponentially with time, then the dynamics is defined as chaotic. The rate at which the trajectories diverge from each other is given by the Lyapunov exponent, $\lambda_L = \lim_{t \rightarrow \infty} \frac{1}{t} \ln \frac{d(t)}{d(0)}$ where $d(t)$ denotes the separation between two classical trajectories at time t . This idea can be easily generalized in a quantum field theory like SU(2), in the semi-classical regime, where the gauge

*Corresponding author, email: sayakg@imsc.res.in

links $U_\mu(\mathbf{x})$ are analogous to the space coordinates in a classical configuration space. Using non-perturbative lattice techniques one can generate ensembles of gauge links using Monte-Carlo algorithms. In thermal equilibrium, two different gauge configurations which are separated by infinitesimal Monte-Carlo time steps can be evolved in real-time using the SU(2) Hamiltonian in order to estimate the Lyapunov exponent.

Alternately the Lyapunov exponent can also be motivated by studying the following out-of-time ordered correlation (OTOC) defined in one-dimensional classical dynamics as,

$$\{x(t), p(0)\}^2 = \left(\frac{\delta x(t)}{\delta x(0)} \right)^2 \sim e^{2\lambda_L t}, \quad (1)$$

The OTOCs can be easily generalized for quantum field theories. For real-valued scalar fields, the expression in the LHS of Eq. 1 in terms of position and momenta can be replaced by a commutator of the field operator $\hat{\phi}(\mathbf{x}, t)$ and their conjugate momentum fields $\hat{\pi}(\mathbf{x}, t)$. However for scalar fields the OTOC can be also equivalently defined as $[\hat{\phi}(\mathbf{x}, t), \hat{\phi}(\mathbf{0}, 0)]^2$ [18]. In a quantum system, OTOC grows exponentially upto some time t_E , called the Ehrenfest time [19] beyond which its growth saturates. This is the timescale beyond which the wavefunction spreads over the entire volume of the system and there is a transition from a wave-like behavior to a particle-like behavior of the quantum system [20]. However in the semi-classical limit, the OTOC will not saturate. Such a scenario is realized when scalar fields have large occupation numbers, where one can replace the commutator with the following expression,

$$C(\mathbf{x}, t) = \langle \{\phi(\mathbf{x}, t), \phi(\mathbf{0}, 0)\}^2 \rangle = \left\langle \left(\frac{\delta \phi(\mathbf{x}, t)}{\delta \pi(\mathbf{0}, 0)} \right)^2 \right\rangle. \quad (2)$$

We henceforth denote the classical fields $\phi(\mathbf{x}, t)$ as $\phi_{\mathbf{x}}(t)$ and similarly for its conjugate fields. If indeed the system is chaotic, the (maximal) Lyapunov exponent λ_L can be extracted from the OTOC using the relation,

$$\lambda_L = \lim_{t \rightarrow \infty} \frac{1}{2t} \ln C(\mathbf{x} = \mathbf{0}, t). \quad (3)$$

An OTOC typically spreads ballistically within the light cone along rays of constant speed $v = x/t$ along the x - t plane with a scaling exponent ν [21] as,

$$C(\mathbf{x}, t) \sim e^{2\lambda(\nu)t}, \quad \lambda(\nu) = \lambda_L \left[1 - \left(\frac{\nu}{v_B} \right)^\nu \right]. \quad (4)$$

From the spectrum of Lyapunov exponents $\lambda(\nu)$ in the velocity space of propagating OTOCs, one can define the butterfly velocity v_B from the relation $\lambda(v_B) = 0$. The quantities λ_L, v_B and exponent ν are all, in general, temperature dependent. In Section 4 we will extract λ_L, v_B for SU(2) gauge theory under thermal equilibrium for a wide range of temperatures as well as in a particular non-equilibrium state. The ab-initio lattice algorithms used for this purpose are detailed in the next section.

3. The algorithm

3.1. Studying highly occupied SU(2) gauge theory under non-equilibrium conditions

For a specific realization of a non-equilibrium state of SU(2) gauge theory we start from an initial condition where the momentum \mathbf{p} modes of the gauge fields are occupied according to a phase-space distribution given by, $\tilde{f}(\mathbf{p}) = g^2 f(\mathbf{p}) = n_0 \frac{Q_s}{|\mathbf{p}|} e^{-\frac{|\mathbf{p}|^2}{2Q_s^2}}$ where Q_s is the gluon-saturation scale which is typically between 1-2 GeV and g is the gauge coupling. We consider $Q_s = 1.5$ GeV in this work. Here and in the subsequent sections we would be considering the theory to be discretized on a 3 dimensional spatial box with N sites along each spatial direction and a is the lattice spacing. The quantity n_0 sets the initial occupation number of the infrared modes of the gauge fields which we have chosen such that it is close to the typical equilibrium energy densities at high temperatures $T > 600$ MeV. Since the occupation numbers are large (owing to g being small), the gauge links behave classically. For generating these classical configurations we solve for the Hamiltonian's equation of motion for the gauge links $U_{\mathbf{x}}(t)$ and its conjugate fields $E_{\mathbf{x}}^{ib}(t)$ along directions $i = 1, 2, 3$ and with color components $b = 1, 2$ on the lattice,

$$\begin{aligned} E_{\mathbf{x}}^{ib} \left(t + \frac{\Delta t}{2} \right) &= E_{\mathbf{x}}^{ib} \left(t - \frac{\Delta t}{2} \right) + 2 \frac{\Delta t}{a} \sum_{j \neq i}^{N^3} \text{tr} \left[i \Gamma^b (V_{\mathbf{x}}^{ij} + c.c.) \right], \\ U_{\mathbf{x}}^i(t + \Delta t) &= e^{i \frac{\Delta t}{a} E_{\mathbf{x}}^{ib} (t + \frac{\Delta t}{2}) \Gamma^b} U_{\mathbf{x}}^i(t), \end{aligned} \quad (5)$$

where Γ^b are generators of SU(2) and $V_{\mathbf{x}}^{ij}$ is the spatial staple defined in the i - j spatial plane as the derivative of the gauge plaquette U_P defined using path ordering \mathcal{P} in color space as,

$$V_{\mathbf{x}}^{ij} = \frac{\delta U_P}{\delta U_{\mathbf{x}}^i}, \quad U_P^{ij} = \mathcal{P} \left(U_{\mathbf{x}}^i U_{\mathbf{x}+\hat{i}}^j U_{\mathbf{x}+\hat{i}+\hat{j}}^{i\ddagger} U_{\mathbf{x}}^{j\ddagger} \right). \quad (6)$$

We use a symplectic leap-frog integrator with a time-step $\Delta t = 0.0125 Q_s$ for the time evolution in order to respect time reversal invariance. We study different lattice volumes with typical extent along the spatial directions $N = 128$, with spacings $a Q_s = 1.115, 0.9, 0.8$ such that the spatial length of the box in physical units is ~ 16 fm. The Gauss law $\frac{d}{dt} \sum_i \text{tr} i \Gamma^a \left[U_{\mathbf{x}}^i(t) - U_{\mathbf{x}+\hat{i}}^i(t) \right]$ was implemented with a precession of 10^{-15} at $t = 0$ and it was checked to remain so at later times. With such a choice of initial condition the system eventually enters a self-similar scaling regime at late times where the gluon distribution function takes the form $\tilde{f}(\mathbf{p}, t) = (Q_s t)^{-4/7} f_s((Q_s t)^{-1/7} \mathbf{p})$, where f_s is a homogeneous function describing a static distribution [22]. Within such a regime the hard (ultraviolet), electric and the magnetic momentum scales, the later two corresponding to scales set by the Debye mass and the square root of the spatial string tension respectively are well separated similar to a thermal plasma [23].

In order to measure the degree of chaoticity in such a system in a gauge-invariant manner, we follow the procedure as outlined in Ref. [15]. First we implement an infinitesimal shift in the initial condition to $n_0 + \delta n_0$ where $\delta n_0 = 10^{-5}$ and perform a Hamiltonian evolution of the gauge links $U_{\mathbf{x}}'(t)$

as a function of time. We next measure the separation between two gauge trajectories at a time t starting with these two infinitesimally close initial conditions through the gauge-invariant distance measure defined in terms of the spatial plaquettes $d(t) = 1/N_P \sum_P |\text{tr}U_P(t) - \text{tr}U'_P(t)|/2$, where N_P are the number of independent plaquettes. We particularly choose the time interval to be within the self-similar scaling regime, in order to extract the Lyapunov exponent.

3.2. Studying thermal $SU(2)$ plasma at high temperatures

At finite temperatures, apart from the hard scale πT present in the problem, there are two new scales that are generated dynamically; the electric scale gT and the magnetic scale $g^2 T/\pi$ [24]. When these three scales are well-separated, one can integrate out the hard and electric gluons, with momenta $\gtrsim gT$ to obtain an effective Hamiltonian [25] which describes the dynamics of the magnetic (soft) gluons where the electric fields \vec{E}_x^i satisfy the equation of motion

$$-\partial_t \vec{E}_x^i + [D_j, \vec{F}^{ji}(\mathbf{x})] = \sigma \vec{E}_x^i + \vec{\zeta}_x^i(t), \quad (7)$$

where σ is the color conductivity and $\vec{\zeta}_x^i(t)$ are the stochastic color-force fields which satisfy $\langle \vec{\zeta}_{\mathbf{x}_1}^{ic}(t_1) \vec{\zeta}_{\mathbf{x}_2}^{jb}(t_2) \rangle = 2T \sigma \delta^{ij} \delta^{cb} \delta^3(\mathbf{x}_1 - \mathbf{x}_2) \delta(t_1 - t_2)$ in accordance to the fluctuation-dissipation relation. Discretizing the Eq. 7, the electric fields, noise fields and color-conductivity can be written in dimensionless units on the lattice in terms of $E_x^i = g \vec{E}_x^i a^2$, $\zeta_x^i = a^3 g \vec{\zeta}_x^i(t)$ and $\sigma a = \frac{\sigma}{T} T a$ respectively. We set σ/T to its perturbative values [26] where the coupling g at each temperature T is determined from the 2-loop β function. We numerically implement Eq. 7 in dimensionless units which is similar to the electric field evolution in Eq. 5 but with additional contributions due to the noise and damping terms given by $-\Delta t/a [a\sigma E_x^{ib}(t - \Delta t) - \zeta_x^{ib}(t - \Delta t)]$. The evolution in Eq. 7 is similar to a Langevin equation of magnetic modes of the gauge fields in presence of a heat bath where the noise term represents the effects of the hard modes which forms the heat-bath and the damping dynamically brings the system to a thermal equilibrium. This classical system consists of $6N^3$ oscillators of energy aT and has an energy density on the lattice [12] given by $\frac{6}{N^3} \sum_{\mathbf{k}} |\mathbf{k}| \frac{aT}{|\mathbf{k}|}$, where the sum is over all allowed lattice momenta \mathbf{k} , which we have also verified in our calculations. On the other hand, the energy density of quantum $SU(2)$ gauge theory at temperatures ~ 2 times than the deconfinement temperature is close to its Stefan-Boltzmann limit $\pi^2 T^4/5$ [27]. The lattice spacing in the effective theory is set in physical units from the criterion that the measured energy density matches with the quantum theory at each T . This results in a condition $T.a = (30/\pi^2)^{1/3}$, which we use to set the lattice spacing in physical units. Once the gauge links are thermalized at a temperature T , there is an onset of a plateau in the values of the plaquette term as a function of Langevin time. We then consider two thermal configurations infinitesimally separated as a function of Langevin time, switch off the noise and the damping terms in the Hamiltonian and evolve them subsequently as a function of real-time. We then calculate the gauge invariant distance measure introduced in the earlier section to calculate the (maximal) Lyapunov exponent.

3.3. Chaotic dynamics near deconfinement phase transition

Near the deconfinement phase transition temperature T_c the hard, electric and the magnetic scales coincide, hence the effective thermal field theory described in the preceding section can no longer describe the gauge field dynamics. Hence we change our strategy to estimate the Lyapunov exponent. Since $SU(2)$ gauge theory shares the same universality class as the 3D Ising model, hence its long-wavelength or low energy critical modes will undergo the same dynamics as a Z_2 scalar field. We thus simulate a relativistic Z_2 scalar field theory to understand the chaotic dynamics of the critical modes near the deconfinement phase transition. We start with the Hamiltonian which on the lattice is defined as,

$$H = \sum_{\mathbf{x}} \left[\frac{\pi_{\mathbf{x}}^2}{2} - \frac{1}{2} \sum_{\mathbf{y} \sim \mathbf{x}} \phi_{\mathbf{x}} \phi_{\mathbf{y}} + \left(\frac{m^2 a^2}{2} + 3 \right) \phi_{\mathbf{x}}^2 + \frac{\lambda_s}{4!} \phi_{\mathbf{x}}^4 \right]. \quad (8)$$

Here $\sum_{\mathbf{y} \sim \mathbf{x}}$ implies the sum over all nearest neighbors \mathbf{y} around the lattice site \mathbf{x} . In our work, we set the values of $m^2 a^2 = -1$, $\lambda_s = 1$. We first generate thermal ensembles using the Langevin algorithm, in which we consider the time evolution of the scalar and its conjugate momentum fields through equations of motion,

$$\partial_t \phi_{\mathbf{x}}(t) = \frac{\partial H}{\partial \pi_{\mathbf{x}}} = \pi_{\mathbf{x}}(t), \quad (9)$$

$$\partial_t \pi_{\mathbf{x}}(t) = -\frac{\partial H}{\partial \phi_{\mathbf{x}}} - \gamma \pi_{\mathbf{x}}(t) + \eta_{\mathbf{x}}(t) \sqrt{2\gamma T}. \quad (10)$$

where γ is the damping term and $\eta_{\mathbf{x}}$ are Gaussian noise fields defined on each lattice site with a zero mean value which satisfies $\langle \eta_{\mathbf{x}}(t) \eta_{\mathbf{y}}(t') \rangle = \delta_{\mathbf{x}\mathbf{y}} \delta(t - t')$. The relation between the damping factor γ and the coefficient of the noise term due to thermal fluctuation can be obtained using the fluctuation-dissipation theorem. To initialize the algorithm we select initial values of $\phi_{\mathbf{x}}(0)$ and $\pi_{\mathbf{x}}(0)$ on each lattice site \mathbf{x} . We then numerically evolve the above differential equations using the symplectic leap-frog algorithm with a time step $\Delta t = 0.01$. After some Langevin time t_L , we expect the system to thermalize since the Langevin algorithm is ergodic and follows the condition of detailed balance. Once we achieve thermalization using the Langevin algorithm, we use the thermal configuration thus obtained, switch off the noise and damping terms and perform a real-time classical evolution of the scalar fields. We also additionally select infinitesimal perturbation about the initial thermal configurations denoted by $\delta \phi_{\mathbf{x}}(0) = 0$ and $\delta \pi_{\mathbf{x}}(0) = r \delta_{\mathbf{x}\mathbf{0}}$, where r is a Gaussian random number between 0-0.01. Since $\delta \pi_{\mathbf{x}}(t) = \partial_t \delta \phi_{\mathbf{x}}(t)$ one can re-express the initial momentum profile in the configuration space at $\mathbf{x} \equiv (0, 0, 0)$, $t = 0$ and then evolve the fluctuations of the scalar field through

$$\partial_t^2 \delta \phi_{\mathbf{x}}(t) = \nabla^2 \delta \phi_{\mathbf{x}}(t) - m^2 \delta \phi_{\mathbf{x}}(t) - \frac{\lambda_s}{2} \phi_{\mathbf{x}}^2(t) \delta \phi_{\mathbf{x}}(t). \quad (11)$$

In the evolution equation Eq. 11 one requires the values of the scalar fields $\phi_{\mathbf{x}}(t)$ which are obtained through a classical Hamiltonian evolution of initial thermalized values of $\phi_{\mathbf{x}}(0)$ at each temperature T , generated earlier using the Langevin algorithm.

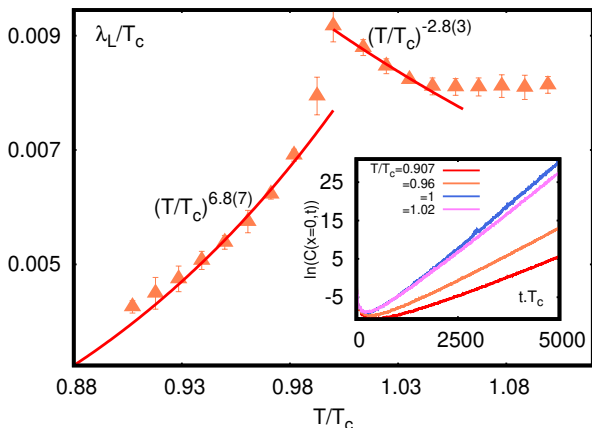


Figure 1: The Lyapunov exponent as a function of T/T_c for a Z_2 scalar field theory which from universality represent the critical long-distance modes of a $SU(2)$ thermal state near the deconfinement temperature T_c . The inset shows the growth of OTOC functions with time $t.T_c$.

We further evolve the initial momentum field fluctuations $\delta\pi_{\mathbf{x}}(t)$ through $\partial_t \delta\phi_{\mathbf{x}}(t) = \delta\pi_{\mathbf{x}}(t)$. We thus have all ingredients to calculate the OTOC function in semiclassical limit using Eq. 2, from which we extract a positive Lyapunov exponent, discussed in the next section.

4. Results

We first measure the OTOC functions for Z_2 scalar field theory at different temperatures close to the phase transition, which is shown in the inset of Fig 1. After an initial dip, The OTOCs exhibit an exponential rise as a function of time. By performing a fit to the OTOCs at late times $t.T_c > 1000$ with an exponential ansatz, we extract the (maximal) Lyapunov exponent at different temperatures, results of which are shown in Figure 1. Here $a.T_c = 9.37$ in dimensionless unit and agrees very well with the values in the literature [28]. The Lyapunov exponent thus extracted varies as $\lambda_L \sim T^{6.8(7)}$ below T_c , whereas in the range $(1, 1.05)T_c$ its temperature variation can be characterized as $T^{-2.8(3)}$, which was determined after performing a fit to our data. The deconfinement phase transition temperature in $SU(2)$ is $T_c \sim 300$ MeV [27].

Further in the inset of Fig 2 we show the heat-map of the OTOC at $T = T_c$ in a two dimensional plane denoted by the time and one of the spatial coordinates, performing a sum over the other spatial coordinates. The OTOC spreads ballistically within the light cone from an initial small perturbation at the origin as evident from the color gradient of the heat-map. In general the λ_L is a function of the velocity and it can be measured from the OTOC function using Eq. 4. As evident in Fig 1, the Lyapunov exponent is maximum along $v = 0$ i.e. along the time direction. We next calculate the butterfly velocity v_B by fitting the OTOC $C(\mathbf{x}, t)$ to the ansatz given in Eq. 4. The v_B varies across the phase transition and is found to be maximum at $T = T_c$. In Fig 2, we have shown the diffusion coefficient as a function of temperature, which is related to the butter-

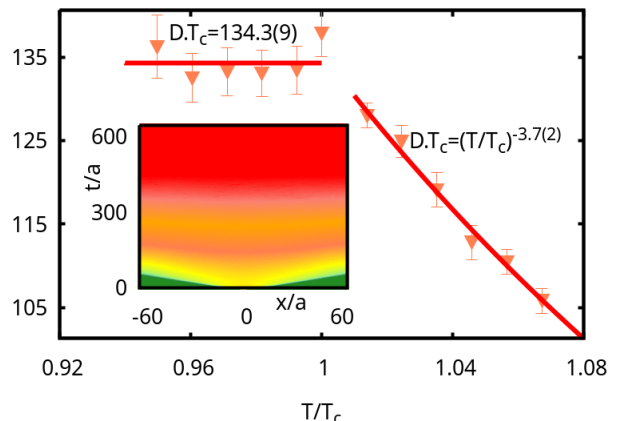


Figure 2: The temperature dependence of the diffusion coefficient D near T_c extracted using Eq. 4. The inset shows the ballistic spread of the OTOC function of Z_2 scalar fields in x - t plane at T_c . The color profile from green to red denotes increasing values of OTOC in the x - t plane.

fly velocity through the relation $D = v_B^2/\lambda_L$ [29]. As evident from the figure, the diffusion coefficient is constant below T_c but decreases with increasing temperatures as $(T/T_c)^{-3.7(2)}$ for $T > T_c$.

At higher temperatures, $T \gg T_c$, the gauge invariant distance measure $d(t) = \frac{1}{2N_p} \sum_P |\text{tr} U_P(t) - \text{tr} U'_P(t)|$ were measured on lattice of $N = 32$ spatial sites and for different temperatures results for which are shown in the inset of Fig 3. The initial $d(t) \sim 10^{-15}$ measures the typical difference between the plaquettes in two thermal configurations which, when evolved in time grows exponentially eventually saturating at late times to $\sim 10^{-2}$, since the trace of plaquette is bounded to unity and the gauge group is compact. The lattice size are chosen large enough for this purpose such that the values are $\sim 15(6)$ fm at temperatures $0.6(1.5)$ GeV respectively. Extracting the (maximal) Lyapunov exponent λ_L from the exponentially rising part of $d(t)$ with time, we study its dependence on temperature, results of which are shown in Fig. 3. The λ_L varies linearly with temperature between 0.6 - 3 GeV with a slope $\lambda_L/T \sim 0.52$ which satisfies the conjectured bound $\lambda_L \leq 2\pi T$ in quantum many-body chaotic systems [30] and also satisfies $\lambda_L \sim g^2 \mathcal{E}/6$, where \mathcal{E} is the average energy per plaquette [11]. The diffusion coefficient extracted from λ_L thus vary inversely with temperature as $(T/T_c)^{-0.95(3)}$ shown in Fig. 4. At these temperatures the distance measure spreads from an initial tiny fluctuation at $t.T = 0$ ballistically over the space-time and grows exponentially within the light-cone, evident from the inset of the same figure, the color gradient from green to red indicates increasing values of the distance measure $d(t)$. Across these high temperatures, the butterfly velocity is $v_B = 0.8c$ and does not vary significantly. Compared to its value at T_c , the butterfly velocity reduces by only $\sim 10\%$ which implies that once thermalized, most of the configuration (color) space gets occupied.

We next extract the Lyapunov exponent within the self-similar scaling regime of the non-equilibrium $SU(2)$ plasma as outlined in Sec. 3.1. In order to compare with a typical ther-

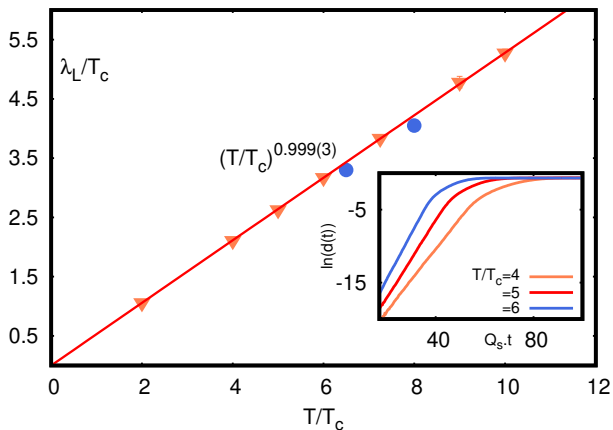


Figure 3: The Lyapunov exponent as a function of T/T_c for a SU(2) gauge theory at high temperatures in thermal equilibrium shown as triangles. These are compared with the Lyapunov exponents in a non-thermal state of SU(2) with comparable energy densities (circles). The inset shows the growth of the gauge invariant distance measure with time $t.T_c$ for the thermal SU(2) state for 3 different temperatures.

mal state at temperature $T \sim 2$ GeV, we set the initial density of gluons to be $n_0 = 16$, and consider lattice box of spatial extent ~ 16 fm such that the energy densities are similar in the thermal as well in the non-thermal scaling regime. The (maximal) Lyapunov exponent $\lambda_L = 0.66 Q_s$ is similar in magnitude to that in a thermal state at $T \gg T_c$. We have also shown the values of the maximal Lyapunov exponents in Fig 3 in this non-thermal state, as a function of an effective temperature which is the fourth root of the energy density, as blue data points. The data points lie on the same curve determining the temperature dependence of the thermal Lyapunov exponents. For lower energy densities $\epsilon (\sim \sqrt{n_0} \lesssim 1)$ it was earlier conjectured [31] and later observed [15] from classical-statistical lattice calculations in the self-similar non-thermal scaling regime of SU(3), that the (maximal) Lyapunov exponent λ_L varies as $\epsilon^{1/4}$. Our calculations were performed in SU(2) non-thermal scaling state at larger gluon energy densities ($\sim \sqrt{n_0} \gtrsim 4$) where we observe a linear scaling of λ_L with ϵ . The linear scaling of λ_L at higher energies similar to a thermal plasma can be understood in terms of linear temperature dependence of the plasmon damping rate [32].

5. Physical implications of our results

Our results demonstrate that the infrared (soft) modes of the SU(2) have chaotic dynamics both in thermal equilibrium at a wide range of temperatures $0.9-10 T_c$ as well in a particular non-thermal fixed point as evident from the positive (maximal) Lyapunov exponent λ_L . Interestingly the λ_L decreases near critical temperature T_c with temperatures $T > T_c$, maximizing at the deconfinement phase transition. Such a property of λ_L for the critical modes has been observed earlier in spin systems [33, 34, 35, 36] as well as in scalar field theories in 2 dimensions [18]. The temperature dependence of λ_L thus,

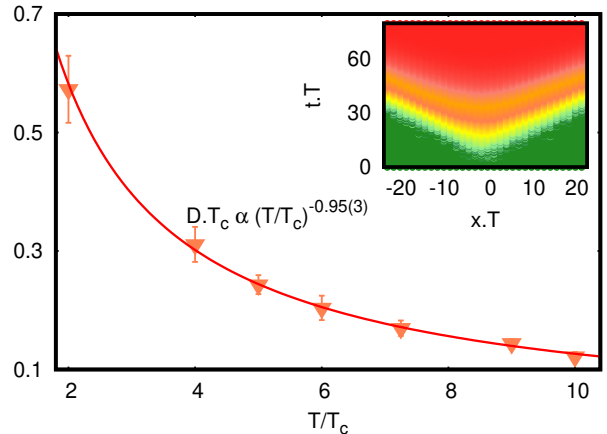


Figure 4: The temperature dependence of the diffusion coefficient D in SU(2) gauge theory at high temperatures $T \gg T_c$. The inset shows the ballistic spread of the Lyapunov exponents in a typical thermal state of SU(2) at $T = 1.2$ GeV. The color gradient from green to red denotes increasing values of OTOC in the $x-t$ plane.

is not particularly related to the details of microscopic interactions between the degrees of freedom but to the symmetries of the system.

The diffusion coefficient D which measures how fast the correlation between the fields increases with time, has many interesting features as a function of temperature. The λ_L at T_c shown in Fig. 1 correspond to the long-wavelength critical modes of SU(2) gauge theory which are a subset of the infrared magnetic modes, whose momenta are bounded by $|\mathbf{p}| \leq g^2 T/\pi$. The fact that D is independent of temperature below and at T_c and decreases sharply above T_c implies that these critical gluon modes at the phase transition are maximally spread in the configuration space. This spread is an inherent chaotic phenomena, which also manifests itself in the stochastic properties [37] of the eigenvalue density of Wilson loop operator in the limit of large number of colors. In this limit, the quantum fluctuations are sub-dominant, and an order-disorder transition [38, 39] in terms of the area of Wilson loops has similar features as the (de)confinement transition.

The temperature dependence of D at $T \gg T_c$ in Fig. 4 can be interpreted from the fact that D represents a diffusion in the configuration space of color gauge links and hence can be related to the inverse of color conductivity σ . The σ calculated perturbatively in a thermal non-Abelian plasma, increases linearly with temperature [26]. In the effective dynamics of the soft (magnetic) modes given in Eq. 7, the σ represent how these modes rearrange in response to the ultra-relativistic hard modes. The soft modes receive random kicks from the thermal bath of hard modes and a finite σ effectively dampens them, allowing for an efficient thermalization.

Next we address the implications of our study for understanding the mechanism of thermalization in gauge theories. When we discuss about thermalization, to be more precise, we imply how fast the magnetic (soft) modes equilibrate. Starting from a non-equilibrium state the entropy increases until it reaches its

maximum in a thermal state. The KS entropy density rate \dot{s}_{KS} can thus be used to estimate the time required in this process. From the sum of all the positive Lyapunov exponents λ_i [9], one can estimate this quantity on the lattice as

$$\dot{s}_{KS} a^4 = -\frac{\sum_i \lambda_i a}{N^3} \sim -4\lambda_L a, \quad (12)$$

for the range of temperatures 2-10 T_c , considering that about 1/3 of $18N^3$ number of the Lyapunov exponents are positive [12] and their values can be obtained from the relation $\lambda(v) \sim \lambda_L [1 - (v/v_B)^2]$ evident in our data, where we have taken the values of v as randomly distributed between 0 and v_B . We have verified that our estimate does not vary significantly if the values of v are chosen to be uniformly distributed between $[0, v_B]$. Starting from a thermal state \dot{s}_{KS} measures the rate at which information about the initial state of the system is lost. We use the thermodynamic relation $s_{th} T = \varepsilon + p$ to obtain the entropy density of a thermal state of SU(2) to be $s_{th} a^3 = \frac{4}{3} \frac{\varepsilon a^4}{T a}$ at temperatures $T \gg T_c$ where the energy density and pressure are related by $\varepsilon \simeq 3p$. On the other hand the entropy density for the non-thermal state in the self-similar regime described in section 3.1, $s_{non-th} a^3 = -\int \tilde{f}(\mathbf{p}) \ln [\tilde{f}(\mathbf{p})] d^3(\mathbf{p}) \simeq 4.8$ can be calculated by performing a numerical integration using the non-thermal distribution f obtained in our computations. Using the entropy densities of the thermal and non-thermal states one can derive the thermalization time $t_{th} = 0.8/\lambda_L(T)$, by integrating over Eq. 12. Thus starting from a highly occupied gluon state in a non-thermal scaling regime, a thermal state at $T \simeq 600$ MeV can be reached within a time, $t_{th} \sim 0.50(3)$ fm/c, whereas it would take $t_{th} \sim 0.70(5)$ fm/c to reach a thermal state at $T \simeq 450$ MeV.

6. Outlook

In this letter, we provide a detailed understanding of the dynamical properties of soft (magnetic) modes of non-Abelian SU(2) gauge theory as a function of temperature as well as in a particular non-thermal attractor state. These magnetic modes interact non-perturbatively even at asymptotically high temperatures [40] and influence dynamical properties like the sphaleron transition rate [25, 41], and other transport properties of the non-Abelian plasma [42]. We show here that these modes play an important role in the process of thermalization in gauge theories. In a high temperature plasma, where a clean separation between the hard (ultraviolet momentum) modes and these soft modes is possible, resulting in an effective stochastic description of the latter [25], we demonstrate the chaotic behavior inherent in the system by extracting the spectra of positive Lyapunov exponents. This allows us to measure the Kolmogorov-Sinai entropy rate which determines how fast the entropy flows into the system eventually attaining a maximum. We have used this rate to measure a thermalization time ~ 0.7 - 0.5 fm/c to reach to a thermal state at 450-600 MeV starting from a particular non-thermal state of soft gluons which shows a particular self-similar behavior [14]. The only assumption that goes into our calculation is the conservation of energy density of the soft

modes during the entire evolution of the system. Interestingly our estimate of the thermalization time is consistent with the early switch-on time of hydrodynamics to describe flow observables in heavy-ion collisions [43] but is smaller than estimates ($\gtrsim 2.5$ fm/c) based on perturbative scattering process [44].

In our approach we can only predict the time taken by the soft modes to thermalize if the initial non-thermal and the final thermal states are known. However understanding the microscopic mechanism that drives the system away from the self-similar non-thermal scaling regime would require a more detailed understanding of how hard particles are created in this regime and how their interactions with the soft modes can be formulated within an effective theory. Possible mechanisms include the onset of plasma instabilities [45, 46, 47, 48, 49, 50, 13, 14, 51], and the process of thermalization is an inherently non-perturbative phenomenon [52]. We would like to address these topics in a future work.

7. Acknowledgements

We are grateful to Sumilan Banerjee, Rajiv Gvai and Soeren Schlichting for discussions related to this work. The authors acknowledge the computing time provided by the High Performance Computing Center at the Institute of Mathematical Sciences.

References

- [1] J. Berges, Introduction to nonequilibrium quantum field theory, AIP Conf. Proc. 739 (1) (2004) 3–62. [arXiv:hep-ph/0409233](#).
- [2] J. Berges, M. P. Heller, A. Mazeliauskas, R. Venugopalan, QCD thermalization: Ab initio approaches and interdisciplinary connections, Rev. Mod. Phys. 93 (3) (2021) 035003. [arXiv:2005.12299](#).
- [3] N. Krylov, J. Migdal, Works on the Foundations of Statistical Physics, Princeton Series in Physics, Princeton University Press, 2014.
- [4] C. E. Shannon, A mathematical theory of communication, The Bell System Technical Journal 27 (3) (1948) 379–423.
- [5] E. T. Jaynes, Information theory and statistical mechanics, Phys. Rev. 106 (1957) 620–630.
- [6] V. Latora, M. Baranger, Kolmogorov-sinai entropy rate versus physical entropy, Phys. Rev. Lett. 82 (1999) 520–523.
- [7] M. Dzugutov, E. Aurell, A. Vulpiani, Universal relation between the kolmogorov-sinai entropy and the thermodynamical entropy in simple liquids, Phys. Rev. Lett. 81 (1998) 1762–1765.
- [8] A. Kolmogorov, Viscosity, black holes, and quantum field theory, Dokl. Akad. Nauk SSSR 119 (1958) 861.
- [9] J. B. Pesin, Ljapunov characteristic exponents and ergodic properties of smooth dynamical systems with an invariant measure, in: Hamiltonian Dynamical Systems, CRC Press, 2020, pp. 512–515.
- [10] G. Savvidy, The yang-mills classical mechanics as a kolmogorov k-system, Physics Letters B 130 (5) (1983) 303–307.
- [11] B. Müller, A. Trayanov, Deterministic chaos in non-abelian lattice gauge theory, Physical review letters 68 (23) (1992) 3387.
- [12] C. Gong, Lyapunov spectra in su (2) lattice gauge theory, Physical Review D 49 (5) (1994) 2642.
- [13] J. Berges, K. Boguslavski, S. Schlichting, R. Venugopalan, Turbulent thermalization process in heavy-ion collisions at ultrarelativistic energies, Phys. Rev. D 89 (7) (2014) 074011. [arXiv:1303.5650](#).
- [14] J. Berges, K. Boguslavski, S. Schlichting, R. Venugopalan, Universal attractor in a highly occupied non-Abelian plasma, Phys. Rev. D 89 (11) (2014) 114007. [arXiv:1311.3005](#).
- [15] H. Pandey, R. Shanker, S. Sharma, Understanding the approach to thermalization from the eigenspectrum of non-Abelian gauge theories (7 2024). [arXiv:2407.09253](#).

- [16] L. Ebner, B. Müller, A. Schäfer, L. Schmotzer, C. Seidl, X. Yao, Entanglement properties of $su(2)$ gauge theory, arXiv preprint arXiv:2411.04550 (2024).
- [17] A. Andronic, P. Braun-Munzinger, K. Redlich, J. Stachel, Decoding the phase structure of QCD via particle production at high energy, *Nature* 561 (7723) (2018) 321–330. arXiv:1710.09425.
- [18] A. Schuckert, M. Knap, Many-body chaos near a thermal phase transition, *SciPost Phys.* 7 (2) (2019) 022. arXiv:1905.00904.
- [19] J. Rammensee, J. D. Urbina, K. Richter, Many-body quantum interference and the saturation of out-of-time-order correlators, *Physical Review Letters* 121 (12) (2018) 124101.
- [20] K. Hashimoto, K. Murata, R. Yoshii, Out-of-time-order correlators in quantum mechanics, *Journal of High Energy Physics* 2017 (10) (2017) 1–31.
- [21] V. Khemani, D. A. Huse, A. Nahum, Velocity-dependent Lyapunov exponents in many-body quantum, semiclassical, and classical chaos, *Phys. Rev. B* 98 (2018) 144304.
- [22] J. Berges, K. Boguslavski, S. Schlichting, R. Venugopalan, Universal attractor in a highly occupied non-abelian plasma, *Physical Review D* 89 (11) (2014) 114007.
- [23] J. Berges, K. Boguslavski, L. de Bruin, T. Butler, J. M. Pawłowski, Order parameters for gauge invariant condensation far from equilibrium, *Phys. Rev. D* 109 (11) (2024) 114011. arXiv:2307.13669.
- [24] M. Laine, A. Vuorinen, *Basics of Thermal Field Theory*, Vol. 925, Springer, 2016. arXiv:1701.01554.
- [25] D. Bodeker, On the effective dynamics of soft nonAbelian gauge fields at finite temperature, *Phys. Lett. B* 426 (1998) 351–360. arXiv:hep-ph/9801430.
- [26] P. B. Arnold, L. G. Yaffe, High temperature color conductivity at next-to-leading log order, *Phys. Rev. D* 62 (2000) 125014. arXiv:hep-ph/9912306.
- [27] J. Fingberg, U. M. Heller, F. Karsch, Scaling and asymptotic scaling in the $SU(2)$ gauge theory, *Nucl. Phys. B* 392 (1993) 493–517. arXiv:hep-lat/9208012.
- [28] D. Schweitzer, S. Schlichting, L. von Smekal, Spectral functions and dynamic critical behavior of relativistic z_2 theories, *Nuclear Physics B* 960 (2020) 115165.
- [29] M. Blake, Universal charge diffusion and the butterfly effect in holographic theories, *Physical review letters* 117 (9) (2016) 091601.
- [30] J. Maldacena, S. H. Shenker, D. Stanford, A bound on chaos, *Journal of High Energy Physics* 2016 (8) (2016) 1–17.
- [31] B. Chirikov, D. Shepelyanski, Stochastic oscillations of classical yamg-mills, *JETP Lett* 34 (4) (1981).
- [32] T. Biró, C. Gong, B. Müller, Lyapunov exponent and plasmon damping rate in non-abelian gauge theories, *Physical Review D* 52 (2) (1995) 1260.
- [33] T. Bilitewski, S. Bhattacharjee, R. Moessner, Temperature dependence of the butterfly effect in a classical many-body system, *Physical review letters* 121 (25) (2018) 250602.
- [34] T. Bilitewski, S. Bhattacharjee, R. Moessner, Classical many-body chaos with and without quasiparticles, *Physical Review B* 103 (17) (2021) 174302.
- [35] S. Ruidas, S. Banerjee, Many-body chaos and anomalous diffusion across thermal phase transitions in two dimensions, *SciPost Physics* 11 (5) (2021) 087.
- [36] P. Butera, G. Caravati, Phase transitions and Lyapunov characteristic exponents, *Physical Review A* 36 (2) (1987) 962.
- [37] J.-P. Blaizot, M. A. Nowak, Large $N(c)$ confinement and turbulence, *Phys. Rev. Lett.* 101 (2008) 102001. arXiv:0801.1859.
- [38] B. Durhuus, P. Olesen, The Spectral Density for Two-dimensional Continuum QCD, *Nucl. Phys. B* 184 (1981) 461–475.
- [39] R. Narayanan, H. Neuberger, Universality of large N phase transitions in Wilson loop operators in two and three dimensions, *JHEP* 12 (2007) 066. arXiv:0711.4551.
- [40] S. Tah, et. al., The spatial string tension and its effects on screening correlators in a thermal QCD plasma (2025). arXiv:to be published.
- [41] G. D. Moore, The Sphaleron rate: Bodeker’s leading log, *Nucl. Phys. B* 568 (2000) 367–404. arXiv:hep-ph/9810313.
- [42] H. B. Meyer, Transport Properties of the Quark-Gluon Plasma: A Lattice QCD Perspective, *Eur. Phys. J. A* 47 (2011) 86. arXiv:1104.3708.
- [43] U. W. Heinz, Thermalization at RHIC, *AIP Conf. Proc.* 739 (1) (2004) 163–180. arXiv:nucl-th/0407067.
- [44] R. Baier, A. H. Mueller, D. Schiff, D. T. Son, Does parton saturation at high density explain hadron multiplicities at RHIC?, *Phys. Lett. B* 539 (2002) 46–52. arXiv:hep-ph/0204211.
- [45] R. Baier, A. H. Mueller, D. Schiff, D. T. Son, ‘Bottom up’ thermalization in heavy ion collisions, *Phys. Lett. B* 502 (2001) 51–58. arXiv:hep-ph/0009237.
- [46] P. B. Arnold, J. Lenaghan, G. D. Moore, QCD plasma instabilities and bottom up thermalization, *JHEP* 08 (2003) 002. arXiv:hep-ph/0307325.
- [47] P. Romatschke, M. Strickland, Collective modes of an anisotropic quark gluon plasma, *Phys. Rev. D* 68 (2003) 036004. arXiv:hep-ph/0304092.
- [48] A. Rebhan, P. Romatschke, M. Strickland, Hard-loop dynamics of non-Abelian plasma instabilities, *Phys. Rev. Lett.* 94 (2005) 102303. arXiv:hep-ph/0412016.
- [49] P. B. Arnold, J. Lenaghan, G. D. Moore, L. G. Yaffe, Apparent thermalization due to plasma instabilities in quark-gluon plasma, *Phys. Rev. Lett.* 94 (2005) 072302. arXiv:nucl-th/0409068.
- [50] A. Kurkela, G. D. Moore, Bjorken Flow, Plasma Instabilities, and Thermalization, *JHEP* 11 (2011) 120. arXiv:1108.4684.
- [51] S. Schlichting, S. Sharma, Chiral Instabilities and the Fate of Chirality Imbalance in Non-Abelian Plasmas, *Phys. Rev. Lett.* 131 (10) (2023) 102303. arXiv:2211.11365.
- [52] Y. V. Kovchegov, Can thermalization in heavy ion collisions be described by QCD diagrams?, *Nucl. Phys. A* 762 (2005) 298–325. arXiv:hep-ph/0503038.